The effects of Na loading on catalytic properties of H$_2$-reduced Pt/MoO$_3$ for heptane isomerization

Hirotoshi Sakagami, Tomoya Ohno, Nobuo Takahashi, Takeshi Matsuda *

Department of Materials Science, Kitami Institute of Technology, 165 Koen-cho, Kitami, Hokkaido 090 8507, Japan

Received 24 December 2005; revised 28 April 2006; accepted 30 April 2006

Available online 9 June 2006

Abstract

Na-loaded MoO$_3$ was reduced with H$_2$ in the presence of Pt, and its catalytic activity for heptane isomerization was studied. The isomerization activity decreased abruptly with increasing Na loading. The same tendency was observed in the dehydration of 2-propanol. In contrast, the catalytic activity for cyclohexene hydrogenation was improved by increasing amounts of Na. The physical properties of the H$_2$-reduced catalysts, such as the surface area and the valence of Mo, were changed very little by the Na content. The isomerization and dehydration activities were related to the concentration of acid sites, which was determined from NH$_3$-TPD. Thus, the isomerization reaction of heptane over H$_2$-reduced Pt/MoO$_3$ is concluded to occur due to the existence of acid sites.

© 2006 Elsevier Inc. All rights reserved.

Keywords: Molybdenum oxide; H$_2$ reduction; Isomerization; Bifunctional property; Acidity

1. Introduction

To boost the octane quality of a gasoline fraction, the refinery industry uses some high-octane components that are paraffinic in nature, such as alkylate and isomerate. These components consist of highly branched isomers and have a relatively low environmental impact. Commercial isomerization catalysts, such as Pt/chlorinated Al$_2$O$_3$, Pt/zeolite, and Pt/SO$_4{}^{2-}$–ZrO$_2$, exhibit high cracking rates when the feedstock contains hydrocarbons with more than 7 carbons, so that this fraction is usually converted to aromatic hydrocarbons in reforming units. From the standpoint of environmental protection, however, aromatic hydrocarbons (especially benzene) should be reduced in gasoline fuel.

After Boudart and coworkers [1–4] reported that oxygen-modified WC behaved as a very efficient catalyst for alkane isomerization, studies on W- and Mo-based isomerization catalysts have been developed with the aim of finding more efficient and cheaper substitutes for the Pt catalysts used in industrial isomerization processes. Ledoux et al. [5–10] reported that hep-

tane isomerization proceeded selectively on oxygen-modified Mo$_2$C and carbon-modified MoO$_3$. On these catalysts, molybdenum oxycarbide (MoO$_x$C$_y$), formed by incorporating carbon atoms in the molybdenum oxide lattice, has been considered the active phase for alkane isomerization. They suggested a bond-shift mechanism via metallocyclic intermediates on MoO$_x$C$_y$ because the catalytic behaviors of MoO$_x$C$_y$ in heptane isomerization differed from those of Pt/Hβ. In the case of oxygen-modified WC, however, a bifunctional mechanism with the dehydrogenation–hydrogenation steps on sites with a metallic character (WC$_x$) and the C–C bond rearrangement steps on acid sites (WO$_x$) has been proposed [1–4].

Mo metal and MoO$_2$ [11], MoO$_2$ alone [12–14], MoO [15,16], and molybdenum oxyhydride (MoO$_x$H$_y$) [17–23] have also been proposed to act as the active phase for alkane isomerization since MoO$_3$ became an active and selective catalyst for isomerization after incomplete reduction with pure H$_2$. The isomerization reaction of alkane on these phases has been considered to proceed via the conventional bifunctional mechanism. As can be seen, the mechanisms at work, as well as the active phase, vary among authors and remain very open.

In the isomerization of alkane over bifunctional catalysts, the balance of the hydrogenation–dehydrogenation function and

---

* Corresponding author. Fax: +81 157 26 4973.

E-mail address: matsutk@mail.kitami-it.ac.jp (T. Matsuda).

the acid function is crucial, because it determines activity, stability, and product selectivity. In previous work [19–23] we showed that the catalytic activity of H_2-reduced Pt/MoO_3 for heptane isomerization depended on the extent of reduction. Its dependency was analogous to that of the 2-propanol dehydration activity, whereas the dehydrogenation activity varied with the extent of reduction in a different way from the isomerization activity. These results indicate that the isomerization activity of H_2-reduced Pt/MoO_3 can be controlled by the ability to act as an acid catalyst. Based on some experimental facts, Meunier suggested that the bifunctional mechanism operated in butane isomerization over H_2-reduced MoO_3, and that the rate-determining step can be the isomerization of n-butene intermediate to iso-butene [24]. H_2-reduced MoO_3 and Pt/MoO_3 were reported to exhibit negative reaction orders toward hydrogen in pentane and heptane isomerization [25,26]. This behavior is a characteristic of alkane isomerization over bifunctional catalysts, such as Pt/zeolites. It is well known that the acidity of a solid acid catalyst is strongly modified by loading of alkali metal. The aims of the present work are to describe the effects of Na loading on the catalytic activity of H_2-reduced Pt/MoO_3 for the isomerization of heptane, and to compare the effects with those for 2-propanol dehydration and cyclohexene hydrogenation.

2. Experimental

2.1. Materials

H_2, N_2, He, and Ar were purified by passage through a molecular sieve and a Mn/SiO_2 oxygen trap. H_2MoO_4 (98% purity) was purchased from Kanto Chemical Co. Commercially available [Pt(NH_3)$_4$]Cl_2 was used without further purification. Heptane, 2-propanol, and cyclohexene (CHE) were dried using a molecular sieve before use. The MoO_3 used in this study was obtained by calcination of H_2MoO_4 at 673 K for 3 h. Na-loaded MoO_3 was prepared by a conventional impregnation method using an aqueous solution of NaCl. Na-loaded MoO_3 is denoted as Na(1)–MoO_3, Na(5)–MoO_3, etc., with the values in parentheses representing the molar percentage of Na. After calcination at 773 K for 6 h, Pt was loaded onto Na–MoO_3 by impregnation using an aqueous solution of [Pt(NH_3)$_4$]Cl_2. The Pt loading was adjusted to be 0.01 wt% for all samples. The Pt-loaded samples were dried overnight at 393 K, then calcined at 773 K for 2 h. The catalyst powders were compressed into flakes, followed by crushing and sieving (30–60 mesh).

2.2. Catalytic tests

Reaction of heptane was carried out at 523–623 K (typically at 523 K) under atmospheric pressure in a conventional fixed-bed flow reactor equipped with a sampling valve for gas chromatographic analysis. A 0.1-g sample of Pt/Na–MoO_3 was packed at the central position of a cell composed of a Pyrex glass tube with an inner diameter of 8 mm. The sample was heated to 773 K at a rate of 5 K/min in a stream of H_2 (60 mL/min) and was kept at that temperature for 1 h. After

H_2 reduction and cooling to reaction temperature in a stream of H_2, heptane was introduced onto the catalyst bed at partial pressure of 9.2 kPa with H_2 as a complement to atmospheric pressure. Reaction of 2-propanol was performed at 398 K and at a molar He/2-P ratio of 20. Reaction conditions of cyclohexene were as follows: temperature = 423 K; H_2/CHE ratio = 20. The composition of effluent gases was analyzed by FID gas chromatography using a TC-1 glass capillary separation column and a Porapak Q separation column.

2.3. Characterization methods

The surface area was determined from the adsorption isotherm of N_2, which was obtained on the sample without exposure to air. The sample was reduced in H_2 flow at 773 K for 1 h, then cooled to room temperature, followed by evacuation for 0.5 h at room temperature. The adsorption isotherm of N_2 was measured at 77 K with a conventional high-vacuum static system. After the adsorption measurement, the reduced sample was heated to 773 K in vacuo, then oxidized to MoO_3 by introducing prescribed amounts of O_2. The average valence of Mo was calculated from the amounts of O_2 consumed in the reoxidation.

Crystalline phases of the H_2-reduced sample were determined by X-ray diffraction (XRD) using Ni-filtered Cu-K_α radiation (PANalytical, X'Pert PRO). The sample for XRD measurements was obtained as follows: Pt/Na–MoO_3 was reduced with H_2 at 773 K for 1 h, followed by flowing N_2 for 0.5 h. After cooling to room temperature under N_2 flow, the reduced sample was transferred to a glove box without exposure to air, then dispersed in a solution of heptane to avoid any bulk oxidation.

Temperature-programmed reduction was carried out to investigate the reducibility of Pt/Na–MoO_3. The 0.4-g sample was treated at 673 K for 1 h in a stream of Ar, then cooled to room temperature. Ar was replaced by a 20% H_2–Ar gas mixture (20 mL/min), followed by heating to 1173 K at a rate of 5 K/min. The concentrations of H_2 and H_2O were monitored with TCD gas chromatography using a Porapak N separation column at 413 K. The acidity of Pt/Na–MoO_3 was determined by temperature-programmed desorption of NH_3. The 0.1-g sample was placed in a quartz tube and reduced at 773 K for 1 h in flowing H_2. After cooling to 373 K and evacuation for 0.5 h, the sample was saturated with NH_3 gas, followed by evacuation for 0.5 h. The temperature of the sample was raised at a rate of 10 K/min to 973 K in a stream of He (50 mL/min, 20 kPa). The change of NH_3 concentration in the gas phase was monitored using an integrated mass spectrometer at $m/e = 16$.

3. Results and discussion

Conversion of heptane was conducted at 523 K under atmospheric pressure. The catalytic activity of H_2-reduced Pt/MoO_3 declined slightly with time on stream; under the reaction conditions used here, the conversion level of heptane on H_2-reduced Pt/MoO_3 was 26% after a 1-h run, and decreased to 21% after a 6-h run. Because the oxidation at 673 K, followed
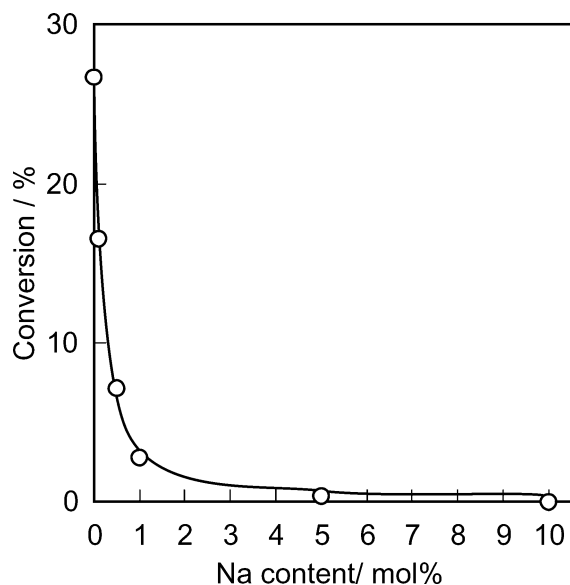
Fig. 1. Catalytic activity of H_2-reduced Pt/Na–MoO$_3$ for the conversion of heptane as a function of the content of Na. Reaction conditions: temperature, 523 K; H_2/C$_7$, 10; W/F, 5 g$_{cat}$ h/C$_7$ mol.
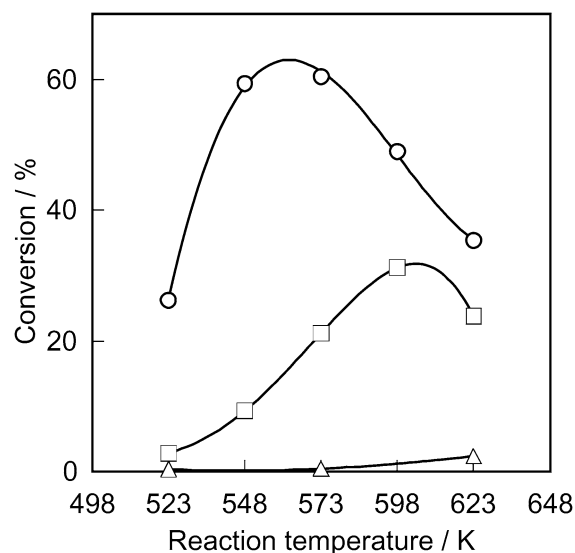

Fig. 2. Effect of reaction temperature on the conversion level of heptane over H_2-reduced Pt/MoO$_3$ (○), Pt/Na(1)–MoO$_3$ (□) and Pt/Na(5)–MoO$_3$ (△). Reaction conditions: H_2/C$_7$, 10; W/F, 5 g$_{cat}$ h/mol.

Table 1
Product distributions in the conversion of heptane

Catalyst	Pt/MoO$_3$	Pt/MoO$_3$	Pt/Na(1)–MoO$_3$
Reaction temp. (K)	523	573	573
Conversion (%)	54.2	53.1	50.3
S_{iso} (%)	97.2	90.9	94.6
Distribution (%)			
Cracking products			
C$_1$	4.1	1.2	11.8
C$_2$	1.4	1.3	5.4
C$_3$	45.1	47.3	35.9
C$_4$	46.1	47.4	36.3
C$_5$	1.7	1.6	5.0
C$_6$	1.6	1.2	5.6
Isomerization products			
2-MH	38.4	39.3	37.6
3-MH	39.8	39.7	41.0
DMP	18.0	18.1	17.6
TMP	3.8	2.9	3.8

conversion level increased with reaction temperature, reaching the maximum value at 548–573 K. Reaction at 598 K and above decreased the conversion level due to the promotion of catalyst deactivation. For H_2-reduced Pt/Na(1)–MoO$_3$, the highest conversion level was obtained at 598 K, although its activity was low compared with that of H_2-reduced Pt/MoO$_3$. In contrast, the reaction of heptane scarcely occurred on H_2-reduced Pt/Na(5)–MoO$_3$ even at 623 K. These results indicate that loading of Na onto MoO$_3$ significantly decreased the catalytic activity.

Product distributions in the conversion of heptane are summarized in Table 1, where the conversion level is adjusted to be about 50%. H_2-reduced Pt/MoO$_3$ catalyzed heptane isomerization very selectively at 523 K. The isomerization selectivity of H_2-reduced Pt/MoO$_3$ decreased to 91% at 573 K. In terms of isomerization selectivity at 573 K, H_2-reduced Pt/Na(1)–MoO$_3$ exhibited higher selectivity than H_2-reduced Pt/MoO$_3$, probably due to its lower acidity. We describe this later in the paper. No appreciable difference in isomerization products was seen among the catalysts tested, but the distribution of cracking products varied with Na loading. Heptane was converted mainly to 2- and 3-methylhexanes in almost equal amounts. C$_3$ and C$_4$ hydrocarbons were formed as the major cracking products on H_2-reduced Pt/MoO$_3$. The selectivities for C$_3$ and C$_4$ were decreased and those for C$_1$, C$_2$, C$_5$, and C$_6$ were increased in the presence of Na. H_2-reduced Pt/Na(1)–MoO$_3$ is likely to catalyze the hydrocracking of heptane and/or its isomerized products.

We reported in previous work [19–23] that H_2 reduction of Pt/MoO$_3$ was accompanied by an increase in surface area, and the catalytic activity for heptane isomerization was strongly dependent on the extent of reduction. Hence, the surface area and the extent of reduction were measured on H_2-reduced Pt/Na–MoO$_3$. As shown in Fig. 3, the surface area changed slightly with Na content. Pt/Na–MoO$_3$ exhibited a larger average valence of Mo than Pt/MoO$_3$ after H_2 reduction at 773 K for 1 h, indicating decreased reducibility of MoO$_3$ in the presence of Na. However, Na loading had very little effect on these properties compared with those on heptane isomerization activity.
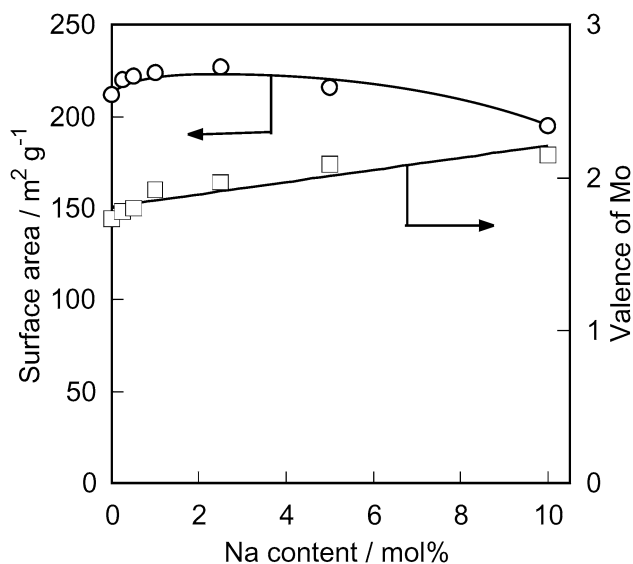
by the reduction at 773 K, regenerated the catalytic activity, coke formation can be the reason for catalyst deactivation. The catalytic activity of Pt/Na–MoO$_3$ also declined with time on stream; for Pt/Na(0.5)–MoO$_3$, the conversion level decreased from 7% after 1 h to 5% after 6 h. The degree of catalyst deactivation varied very little with Na loading; hence, the catalytic activity was compared using data obtained after a 1-h run.

Fig. 1 shows the catalytic activity of H_2-reduced Pt/Na–MoO$_3$ as a function of Na content. The catalytic activity decreased abruptly with increasing content of Na. The catalysts with Na content >5 mol% were almost inactive for the conversion of heptane. The effects of reaction temperature on heptane conversion are shown in Fig. 2. On H_2-reduced Pt/MoO$_3$, the

Fig. 3. Effect of the content of Na on the surface area (○) and the valence of Mo (□) in H_2-reduced Pt/Na–MoO_3.

Fig. 4. Catalytic activity of H_2-reduced Pt/Na–MoO_3 for the conversion of 2-propanol as a function of the content of Na. Reaction conditions: temperature, 398 K; He/2-P, 20; W/F, 5 g_{cat} h/mol.
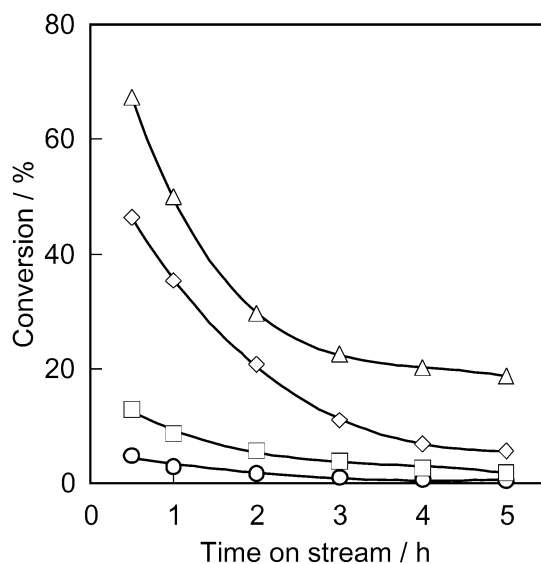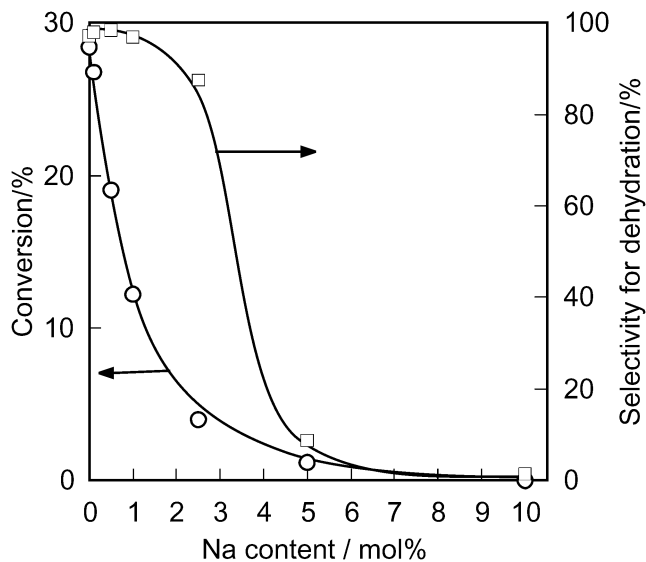

Fig. 5. Effect of the content of Na on the catalytic activity of H_2-reduced Pt/Na–MoO_3 for the conversion of cyclohexene. Na content (mol%): (○) 0; (□) 1; (△) 5; (◇) 10. Reaction conditions: temperature, 423 K; H_2/CHE, 20; W/F, 5 g_{cat} h/mol.

Fig. 6. Variation in the yields of CHA (○, □) and MCP (△, ◇) with the conversion level of CHE on H_2-reduced Pt/MoO_3 (○, △) and Pt/Na(5)–MoO_3 (□, ◇). Reaction conditions: temperature, 423 K; H_2/CHE, 20.

In the isomerization of alkane over bifunctional catalysts, balance between the hydrogenation–dehydrogenation function and the acid function is crucial, because it determines activity, stability, and product selectivity. To study the effects of Na loading on the bifunctional property of H_2-reduced Pt/Na–MoO_3, the reactions of 2-propanol dehydration and cyclohexene (CHE) hydrogenation were performed. Catalyst deactivation in the conversion of 2-propanol was almost similar to that in heptane isomerization. Hence, the catalytic activity was compared using data obtained after a 1-h run. Fig. 4 shows the effects of Na loading on the catalytic properties for the conversion of 2-propanol. The conversion level decreased markedly with increasing Na content. The catalysts with >5 mol% Na were almost inactive for the conversion of 2-propanol. Under
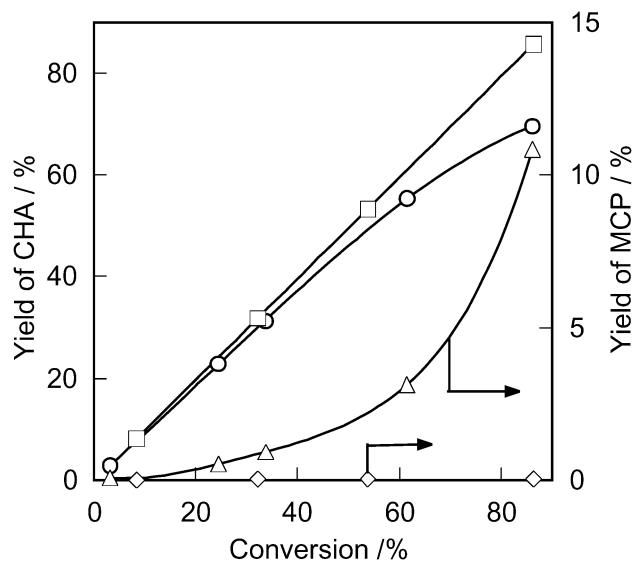
the reaction conditions used here, 2-propanol was converted to propene and diisopropylether by dehydration and to acetone by dehydrogenation. As shown in Fig. 4, 2-propanol was selectively dehydrated on the catalysts with ⩽2.5 mol% Na. The effect of Na loading on dehydration activity is very similar to that on isomerization activity.

Results of the reaction of CHE are shown in Fig. 5. The H_2-reduced Pt/Na–MoO_3 was significantly deactivated in the conversion of CHE. The catalytic activity was increased by Na loading, with the greatest activity obtained on Pt/Na(5)–MoO_3. The formation of cyclohexane (CHA) and methylcyclopentane (MCP) was observed in the conversion of CHE. As shown in Fig. 6, H_2-reduced Pt/MoO_3 yielded CHA selectively at low
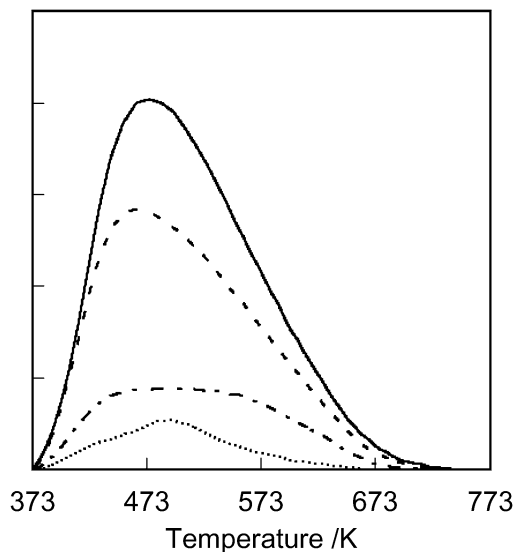
Fig. 7. NH$_3$-TPD spectra of H$_2$-reduced Pt/MoO$_3$ (—), Pt/Na(1)–MoO$_3$ (- - -), Pt/Na(5)–MoO$_3$ (-·-·), and Pt/Na(10)–MoO$_3$ (······).

Fig. 8. The concentration of acid sites over H$_2$-reduced Pt/Na–MoO$_3$ as a function of the content of Na.

conversion levels and yielded the mixture of CHA and MCP at high conversion levels, indicating the isomerization of CHA to MCP. In contrast, no MCP detected in the product on H$_2$-reduced Pt/Na(5)–MoO$_3$ even at high conversion levels. It is well known that both the metal function and the acid function are required for CHA conversion to MCP. Thus, these results suggest that H$_2$-reduced Pt/MoO$_3$ had both the acidic and metallic properties, whereas H$_2$-reduced Pt/Na(5)–MoO$_3$ had no acidity to convert CHA to MCP. The results obtained in the conversions of 2-propanol and CHE allow us to propose that the low catalytic activity of Pt/Na–MoO$_3$ for heptane isomerization can be related to its acidity.

Temperature-programmed desorption of NH$_3$ (NH$_3$-TPD) was carried out to study the acidity of the H$_2$-reduced catalysts. Typical results are shown in Fig. 7. No desorption of NH$_3$ occurred from the catalysts without H$_2$ reduction. NH$_3$ was desorbed in the temperature range of 373–673 K from all of the catalysts tested, but the amount of desorbed NH$_3$ depended on the Na content. The concentration of acid sites was determined from the NH$_3$-TPD spectra. As shown in Fig. 8, there was a good relationship between the concentration of acid sites and Na content, indicating that the generation of acid sites by H$_2$ reduction was retarded in the presence of Na.

The catalytic results shown in Figs. 1 and 4 were represented as a function of the concentration of acid sites. Typical results are shown in Fig. 9. The catalysts with acid sites of ≤0.1 mmol/g were inactive for both heptane isomerization and 2-propanol dehydration. At acid amounts above this value, the rate of 2-propanol dehydration was linearly raised by an increase in acid amount. In the case of heptane isomerization, the reaction rate was slightly enhanced by increasing acid sites, and a sharp upturn in the isomerization rate appeared at acid sites of about 0.2 mmol/g. It was shown in previous papers [22,26] that the amount of Pt loading in the range of 0.001–0.1% had no effect on the rates of pentane and heptane isomerization over H$_2$-reduced Pt/MoO$_3$, whereas the catalytic activities for
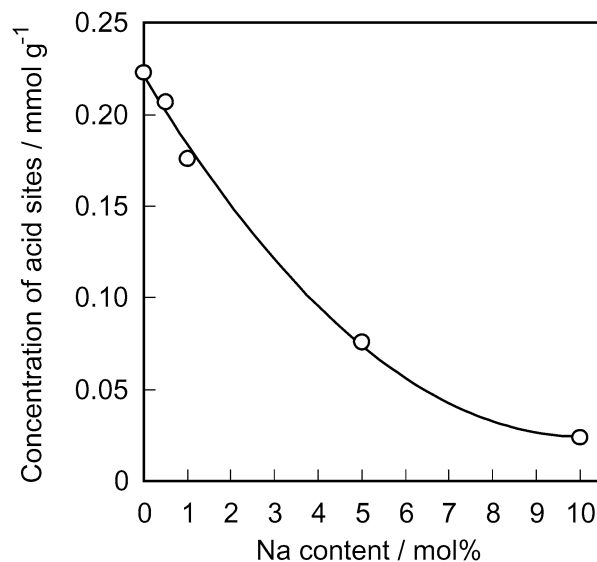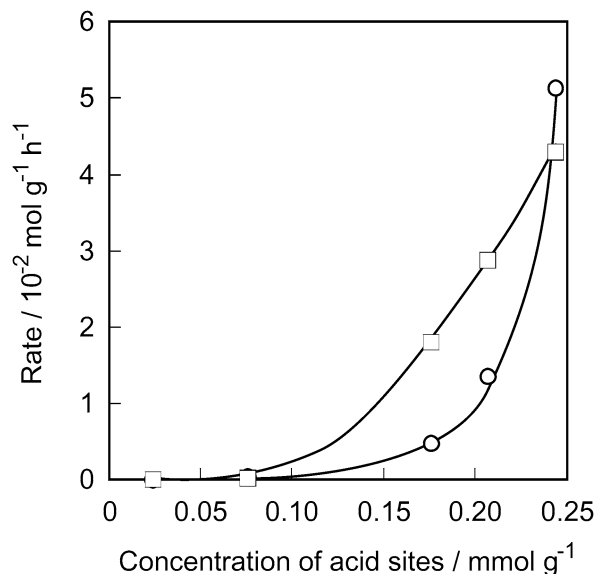

Fig. 9. Effect of the concentration of acid sites on the rates of heptane isomerization (○) and 2-propanol dehydration (□) over H$_2$-reduced Pt/Na–MoO$_3$.

benzene hydrogenation and 2-propanol dehydrogenation were improved by increased Pt content. These results indicate that the dehydrogenation/hydrogenation steps do not control the isomerization rate. Based on these results, we suggest that the low acidity of H$_2$-reduced Pt/Na–MoO$_3$ was responsible for its low activity for heptane isomerization, although a linear relationship between them was not observed. In general, the rates of acid-catalyzing reactions are influenced by the type of acid sites (Brønsted or Lewis sites), as well as by the acid amount. Thus, the type of acid sites seems to vary with the content of Na, and the isomerization reaction can be more sensitive to the acid type than the dehydration reaction. This will be described in a future paper.

Fig. 10 illustrates the XRD diagrams of the catalysts reduced with H$_2$ at 773 K for 1 h. H$_2$-reduced Pt/MoO$_3$ provided
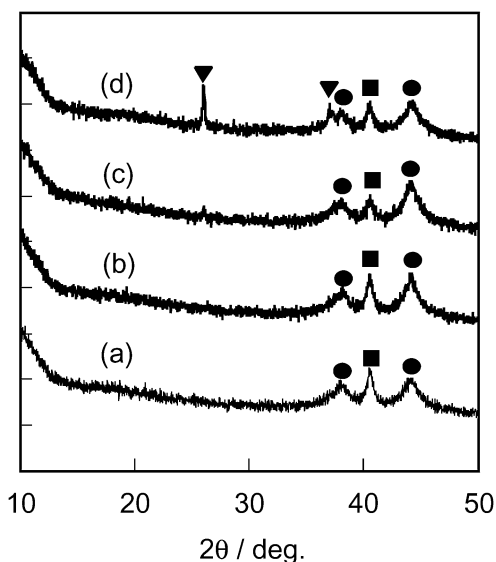
Fig. 10. XRD patterns of Pt/Na–MoO$_3$ reduced at 773 K for 1 h. Na content (mol%): (a) 0; (b) 1; (c) 5; (d) 10. MoO$_2$ (▼), MoO$_x$H$_y$ (●), Mo metal (■).

diffraction lines at $2\theta = 38.1°$, $40.5°$, and $44.3°$. The line at $2\theta = 40.1°$ is assigned to $d(001)$ diffraction of the Mo metal phase. The formation of a nonidentified compound, with diffraction lines appearing at around $38°$ and $44°$, was observed in the reduction products of MoO$_3$ and Pt/MoO$_3$. Hawkins and Worrel assigned these diffraction lines to a Mo$_2$O oxide [27]. MoO with a face-centered cubic lattice was also proposed to account for the XRD pattern [28,29]. Ledoux et al. [7] attributed them to the molybdenum oxyhydride (MoO$_x$H$_y$) phase, which is analogous to molybdenum oxycarbide (MoO$_x$C$_y$). We have also considered that these lines may reflect the formation of MoO$_x$H$_y$, because H$_2$-reduced MoO$_3$ and Pt/MoO$_3$ containing this phase were active for 2-propanol dehydration [17,20–22]. In contrast, Wehrer and co-workers [15,16] pointed out that the presence of hydrogen in this compound was hardly accepted, because thermal treatment at 973 K in a flow of He did not change the XRD pattern, and proposed the existence of a reduced molybdenum oxide with composition close to MoO. We reported previously [30] that the evolution H$_2$O appeared during thermal treatment of H$_2$-reduced MoO$_3$, which was active for 2-propanol dehydration, even though the XRD pattern changed very little. This fact indicates the presence of hydrogen in the reduction product. Thus, this compound is referred to as MoO$_x$H$_y$ in this study, although the nature of this compound varies among different authors and is still under discussion. H$_2$-reduced Pt/Na(1)–MoO$_3$and Pt/Na(5)–MoO$_3$ provided the same XRD patterns as H$_2$-reduced Pt/MoO$_3$. In contrast, the diffraction lines corresponding to the MoO$_2$ phase, as well as those corresponding to the MoO$_x$H$_y$ and Mo metal phases, appeared in H$_2$-reduced Pt/Na(10)–MoO$_3$.

TPR was performed to study the reduction processes of Pt/MoO$_3$, Pt/Na(5)–MoO$_3$, and Pt/Na(10)–MoO$_3$. Fig. 11 depicts the profiles of H$_2$ consumption and of H$_2$O formation during TPR in a 20% H$_2$–Ar gas mixture. Pt/MoO$_3$ reacted with H$_2$ without generation of an equivalent amount of H$_2$O in the low-temperature region, indicating the formation of hydrogen
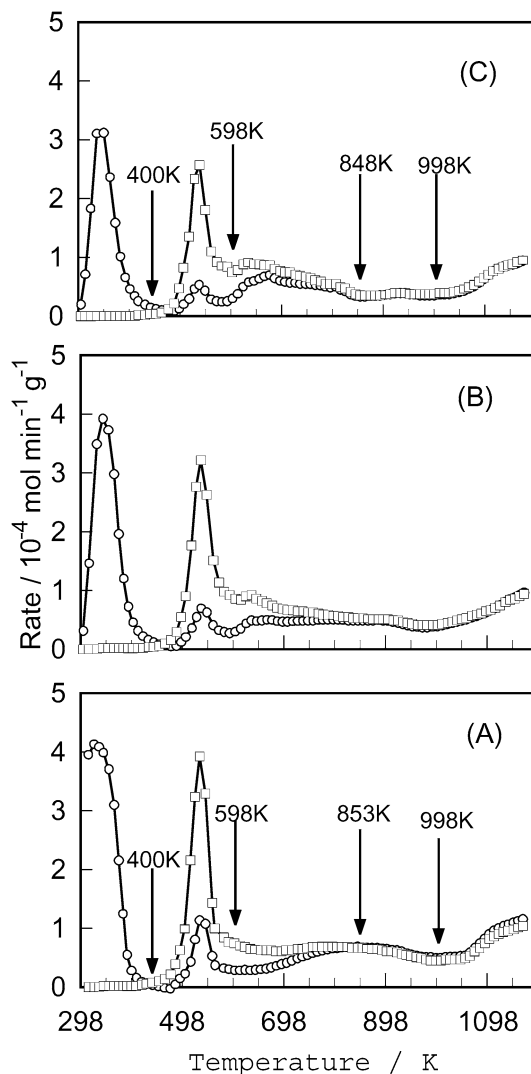

Fig. 11. TPR spectra of Pt/MoO$_3$ (A), Pt/Na(5)–MoO$_3$ (B), and Pt/Na(10)–MoO$_3$ (C). H$_2$ (○), H$_2$O (□). Conditions: sample weight, 0.4 g; gas, 20% H$_2$–Ar; flow rate, 20 mL/min; heating rate, 5 K/min.

molybdenum bronze, H$_x$MoO$_3$. This phenomenon can be understood by considering hydrogen spillover. A large amount of H$_2$O was evolved compared with the amount of H$_2$ reacted in the range of 400–600 K. This implies that the decomposition of H$_x$MoO$_3$ proceeded in this temperature range. At higher temperatures, very broad peaks appeared, and the amount of H$_2$ reacted was consistent with the amount of H$_2$O formed. The TPR profiles of Pt/Na(5)–MoO$_3$ and Pt/Na(10)–MoO$_3$ below 598 K were analogous to the TPR profile of Pt/MoO$_3$, but the amount of H$_2$ reacted in this temperature region varied with the amount of Na loading; the amounts of H$_2$ reacted with Pt/MoO$_3$, Pt/Na(5)–MoO$_3$, and Pt/Na(10)–MoO$_3$ were calculated from the TPR spectra as 6.0×10^{-3}, 4.3×10^{-3}, and 3.4×10^{-3} mol/g$_{MoO_3}$, respectively. Pt/Na(5)–MoO$_3$ gave a small peak at about 645 K. In Pt/Na(10)–MoO$_3$, this peak grew larger and appeared at around 698 K.

Fig. 12 shows the XRD patterns of Pt/MoO$_3$ and Pt/Na(10)–MoO$_3$ used for the TPR measurements. These samples were obtained from the separate experiments. Pt/MoO$_3$ heated to 400 K
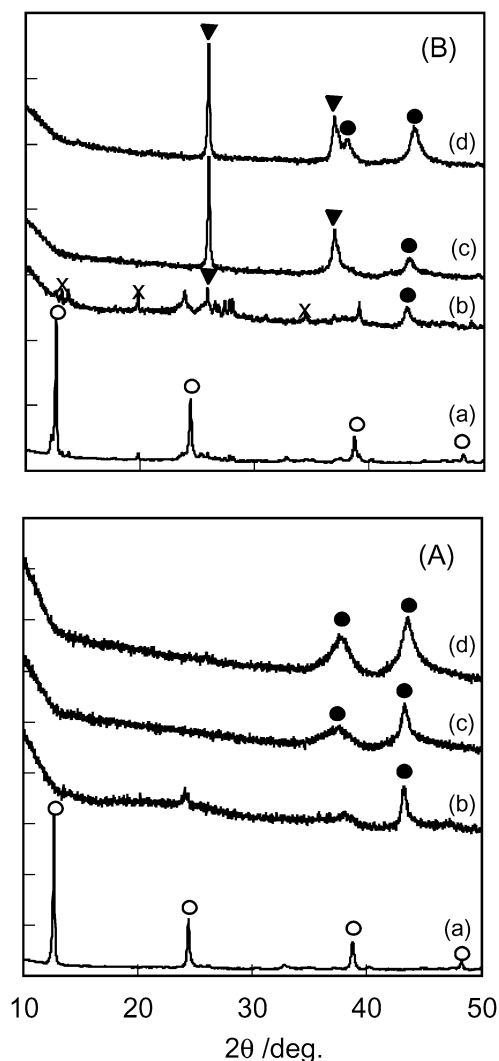
Fig. 12. XRD patterns of Pt/MoO$_3$ (A) and Pt/Na(10)–MoO$_3$ (B) used for TPR. (a) 400 K; (b) 598 K; (c) 853 K in (A) and 848 K in (B); (d) 998 K. H$_{1.68}$MoO$_3$ (○), MoO$_2$ (▼), MoO$_x$H$_y$ (●), MoOCl$_3$ (×).

gave no diffraction peaks due to the MoO$_3$ phase, and the lines corresponding to the H$_{1.68}$MoO$_3$ phase appeared. This result is in accordance with the TPR results (Fig. 11), with the value of x in H$_x$MoO$_3$ determined to be 1.72 from the TPR results. The H$_{1.68}$MoO$_3$ phase disappeared completely, and the MoO$_x$H$_y$ phase was detected at 598 K. The intensity of these diffraction lines was strengthened with increasing reduction temperature from 598 to 998 K. Based on this finding, we suggest that reduction to MoO$_x$H$_y$ occurred mainly in this temperature range in TPR, although the small peak corresponding to the MoO$_x$H$_y$ phase appeared after heating to 598 K. As shown in Fig. 12B, the H$_{1.68}$MoO$_3$ phase was formed even in Pt/Na(10)–MoO$_3$ after heating to 400 K. Pt/Na(10)–MoO$_3$ heated to 598 K gave the diffraction lines due to the MoO$_2$, MoO$_x$H$_y$, and MoOCl$_3$ phases with nonidentified diffraction lines. The formation of MoO$_2$ was promoted by an increase in reduction temperature from 598 to 848 K, indicating that the broad peak observed at around 698 K in TPR can result from reduction to MoO$_2$. The diffraction lines due to MoO$_x$H$_y$ were enlarged after heating to

998 K. The formations of H$_{1.68}$MoO$_3$ and MoO$_2$ were also observed in the Pt/Na(5)–MoO$_3$ used for TPR, although reduction with pure H$_2$ at 773 K for 1 h did not yield the MoO$_2$ phase (Fig. 10). It is obvious from the XRD results that Na loading affected the reduction process. Pt/MoO$_3$ was reduced through the formation of H$_{1.68}$MoO$_3$ without MoO$_2$, but reduction of Pt/Na–MoO$_3$ involved the formation of MoO$_2$.

The average valences of Mo in Pt/MoO$_3$, Pt/Na(5)–MoO$_3$, and Pt/Na(10)–MoO$_3$ heated to 1173 K in TPR were determined to be 2.4, 2.8, and 3.0, respectively, based on the amounts of H$_2$ consumed. This result indicates that reduction of Pt/MoO$_3$ and Pt/Na–MoO$_3$ proceeded more slowly under the TPR condition compared with that under pure H$_2$ flow (Fig. 3). We have reported in previous work [34,35] that MoO$_3$ was more deeply reduced at the higher H$_2$ flow rate because the water vapor generated by the reduction reaction itself inhibited the reduction of molybdenum oxides. Wehrer et al. reported the same result [16]. The ratios of H$_2$ flow rate and catalyst weight in reduction under pure H$_2$ and in TPR were 600 mL/g and 10 mL/g, respectively. Thus, the partial pressure of the water became much greater in TPR, resulting in suppression of the reduction reaction.

In TPR, H$_{1.68}$MoO$_3$ was formed in all of the catalysts (Fig. 12), but the amounts of H$_2$ reacted in the low-temperature region varied with Na content. This implies that the degree of MoO$_3$ conversion to H$_{1.68}$MoO$_3$ was dependent on Na content. The TPR results show the complete conversion of MoO$_3$ to H$_{1.68}$MoO$_3$ in Pt/MoO$_3$. For Pt/Na(5)–MoO$_3$ and Pt/Na(10)–MoO$_3$, the conversion of MoO$_3$ to H$_{1.68}$MoO$_3$ was calculated as 74 and 58%, respectively, from the TPR results. Ledoux et al. [9] reported that treatment of hydrogen molybdenum bronze, H$_{0.34}$MoO$_3$, prepared using MoO$_3$, Zn metal, and an aqueous solution of HCl with a gas mixture of H$_2$ and hydrocarbon, provided molybdenum oxycarbide (MoO$_x$C$_y$) as a pure phase, whereas the mixture of MoO$_x$C$_y$ and MoO$_2$ was obtained from MoO$_3$. The same results were obtained in molybdenum oxyhydride (MoO$_x$H$_y$) [23,31]. Our previous paper shows that formation of the MoO$_2$ phase was not detected by XRD in H$_2$-reduced Pt/MoO$_3$ with a Mo valence of 4.0–1.0 when the MoO$_3$ phase was completely converted to the H$_{1.68}$MoO$_3$ phase [20]. Thus, the formation of MoO$_2$ in Pt/Na(5)–MoO$_3$ and Pt/Na(10)–MoO$_3$ likely results from the incomplete conversion of MoO$_3$ to H$_{1.68}$MoO$_3$.

We reported in previous work [21,32] that Pt/MoO$_3$ was converted to MoO$_2$ without the formation of H$_{1.68}$MoO$_3$ when reduction was performed at 673 K and above after heating in N$_2$ flow. As shown in Figs. 11 and 12, H$_{1.68}$MoO$_3$ decomposed at 400–598 K, indicating that H$_{1.68}$MoO$_3$ was unstable at temperatures above 598 K. Bond and Tripathi have also reported that hydrogen bronze of molybdenum begins to dehydrate above 473 K [33]. These results demonstrate that H$_{1.68}$MoO$_3$ cannot be formed from MoO$_3$ at temperatures above 673 K because of its low thermal stability. When the reduction involved the formation of MoO$_2$, H$_2$-reduced Pt/MoO$_3$ exhibited very low activities for heptane isomerization and 2-propanol dehydration. Wehrer and coworkers [15,16] reported that MoO$_2$ alone, as well as MoO$_2$ associated with Mo metal, were very inef-

ficient catalysts for the skeletal isomerization of alkane and alkene. The results obtained in this study were consistent with the reported results. H_2-reduced Pt/Na(10)–MoO_3 contained the MoO_2 phase, and its activities for heptane isomerization and 2-propanol dehydration were very low. Based on these results, we propose that the reduction involving the formation of MoO_2 can be a cause of the low acidity of H_2-reduced Pt/Na–MoO_3, and the generation of acid sites can be related to the reduction of $H_{1.68}MoO_3$ to MoO_xH_y. As shown in Fig. 5, the hydrogenation activity changed greatly with Na content, indicating that the metallic character as well as the acidity was influenced by the amount of Na loading. The effects of Na loading on the metallic function of H_2-reduced Pt/MoO_3 will be described in a future paper.

4. Conclusion

The effects of Na loading on the catalytic activities of H_2-reduced Pt/MoO_3 for reactions of heptane, 2-propanol, and cyclohexene were studied. The catalytic activities for heptane isomerization and 2-propanol dehydration decreased abruptly with increasing Na loading, whereas the hydrogenation activity for cyclohexene was improved by an increase in Na content. The NH_3-TPD results indicated that the generation of acid sites by H_2 reduction was retarded in the presence of Na, and the low acidity of H_2-reduced Pt/Na–MoO_3 was responsible for its low activity for heptane isomerization and 2-propanol dehydration. TPR and XRD studies showed that the formation of hydrogen bronze of molybdenum, $H_{1.68}MoO_3$, was retarded in the presence of Na, and that reduction of Pt/Na–MoO_3 involved the formation of MoO_2. These results allow us to propose that the low acidity of H_2-reduced Pt/Na–MoO_3 can result from a reduction process involving the formation of MoO_2, and that the reduction of $H_{1.68}MoO_3$ to MoO_xH_y can be accompanied by the generation of acid sites.

Acknowledgments

References

[1] F.H. Ribeiro, R.A. Dalla Betta, M. Boudart, J.E. Baumgartner, E. Iglesia, J. Catal. 130 (1991) 86.
[2] F.H. Ribeiro, M. Boudart, R.A. Dalla Betta, E. Iglesia, J. Catal. 130 (1991) 498.
[3] E. Iglesia, J.E. Baumgartner, F.H. Ribeiro, M. Boudart, J. Catal. 131 (1991) 523.
[4] E. Iglesia, F.H. Ribeiro, M. Boudart, J.E. Baumgartner, Catal. Today 15 (1992) 307.
[5] E.A. Blekkam, C. Pham-Huu, M.J. Ledoux, J. Guille, Ind. Eng. Chem. Res. 33 (1994) 1657.
[6] M.J. Ledoux, C. Pham-Huu, P. Delporte, E.A. Blekkam, A.P.E. York, E.G. Derouane, A. Fonseca, Stud. Surf. Sci. Catal. 92 (1994) 81.
[7] P. Delporte, F. Meunier, C. Pham-Huu, P. Vennegues, M.J. Ledoux, J. Guille, Catal. Today 23 (1995) 251.
[8] A.P.E. York, C. Pham-Huu, P.D. Gallo, E.A. Blekkam, M.J. Ledoux, Ind. Eng. Chem. Res. 35 (1996) 672.
[9] C. Bouchy, C. Pham-Huu, B. Heinrich, C. Chaumont, M.J. Ledoux, J. Catal. 190 (2000) 92.
[10] C. Bouchy, C. Pham-Huu, B. Heinrich, E.G. Derouane, S.B. Derouane-Abd Hamid, M.J. Ledoux, Appl. Catal. A 215 (2001) 175.
[11] R. Burch, P.C.H. Mitchell, J. Less-Common Metals 54 (1977) 363.
[12] A. Katrib, P. Leflaive, L. Hilaire, G. Maire, Catal. Lett. 38 (1996) 95.
[13] A. Katrib, A. Benadda, J.W. Sobczak, G. Maire, Appl. Catal. A 242 (2003) 31.
[14] A. Benadda, A. Katrib, A. Barama, Appl. Catal. A 251 (2003) 93.
[15] P. Wehrer, S. Libs, L. Hilaire, Appl. Catal. A 238 (2003) 69.
[16] P. Wehrer, L. Hilaire, E. Petit, Appl. Catal. A 273 (2004) 249.
[17] T. Matsuda, Y. Hirata, H. Sakagami, N. Takahashi, Microporous Mesoporous Mater. 42 (2000) 345.
[18] T. Matsuda, Y. Hirata, S. Suga, H. Sakagami, N. Takahashi, Appl. Catal. A 193 (2000) 185.
[19] F. Uchijima, T. Takagi, H. Itoh, T. Matsuda, N. Takahashi, Phys. Chem. Chem. Phys. 2 (2000) 1077.
[20] T. Matsuda, F. Uchijima, H. Sakagami, N. Takahashi, Phys. Chem. Chem. Phys. 3 (2001) 4430.
[21] T. Matsuda, H. Sakagami, N. Takahashi, Catal. Today 81 (2003) 31.
[22] T. Matsuda, S. Uozumi, N. Takahashi, Phys. Chem. Chem. Phys. 6 (2004) 665.
[23] T. Matsuda, Y. Asano, H. Sakagami, N. Takahashi, Chem. Lett. 32 (2003) 556.
[24] F.C. Meunier, Chem. Commun. 15 (2003) 1954.
[25] T. Matsuda, K. Watanabe, H. Sakagami, N. Takahashi, Appl. Catal. A 242 (2003) 267.
[26] T. Matsuda, H. Kodama, H. Sakagami, N. Takahashi, Appl. Catal. A 248 (2003) 269.
[27] D.T. Hawkins, W.L. Worrel, Metall. Trans. 1 (1970) 271.
[28] M. Saito, R.B. Anderson, J. Catal. 63 (1980) 438.
[29] D. Wang, D.S. Su, R.Z. Schlogl, Anorg. Allg. Chem. 630 (2004) 1007.
[30] T. Matsuda, H. Sakagami, N. Takahashi, Appl. Catal. A: Gen. 213 (2001) 83.
[31] H. Sakagami, Y. Asano, N. Takahashi, T. Matsuda, Appl. Catal. A: Gen. 284 (2005) 123.
[32] T. Matsuda, A. Hanai, F. Uchijima, H. Sakagami, N. Takahashi, Microporous Mesoporous Mater. 51 (2002) 155.
[33] G.C. Bond, J.B. Tripathi, J. Chem. Soc., Faraday Trans. 1 72 (1976) 933.
[34] T. Matsuda, Y. Hirata, F. Uchijima, H. Itoh, N. Takahashi, Bull. Chem. Soc. Jpn. 73 (2000) 1029.
[35] T. Matsuda, A. Hanai, F. Uchijima, H. Sakagami, N. Takahashi, Bull. Chem. Soc. Jpn. 75 (2002) 1165.